

## LONG-TERM X-RAY MONITORING OF 1E 1740.7–2942 AND GRS 1758–258

D. S. MAIN,<sup>1</sup> D. M. SMITH,<sup>1</sup> W. A. HEINDL,<sup>2</sup> J. SWANK,<sup>3</sup> M. LEVENTHAL,<sup>4</sup>  
I. F. MIRABEL,<sup>5</sup> AND L. F. RODRÍGUEZ<sup>6</sup>

Received 1999 March 8; accepted 1999 July 2

### ABSTRACT

We report on long-term observations of the Galactic bulge black hole candidates 1E 1740.7–2942 and GRS 1758–258 made with the *Rossi X-Ray Timing Explorer*; 1E 1740.7–2942 has been observed 77 times and GRS 1758–258 has been observed 82 times over the past 1000 days. The flux of each object has varied by no more than a factor of 2.5 during this period, and the indices of the energy spectra have varied by no more than 0.4. The power spectra are similar to other black hole candidates: flat-topped noise, breaking to a power law. Each object has exhibited a brightening that lasted for several months, and we have found a time lag between the photon power-law index and the count rate. In both sources, the spectrum is softest during the decline from the brightening. This behavior can be understood in the context of thin-disk and advection-dominated accretion flows coexisting over a wide range of radii, with the implication that both sources have low-mass companions and accrete via Roche lobe overflow.

*Subject headings:* accretion, accretion disks — black hole physics —  
stars: individual (1E 1740.7–2942, GRS 1758–258) — X-rays: stars

### 1. INTRODUCTION

Black hole candidates 1E 1740.7–2942 and GRS 1758–258 are by far the brightest persistent sources in the Galactic bulge above  $\sim 50$  keV (Sunyaev et al. 1991). Their spectra are typical of a black hole low (hard) state (Heindl et al. 1993; Sunyaev et al. 1991). Although variable over times of days to years, they spend most of their time near their brightest observed level. Both have a core/jet structure in the radio (Heindl, Prince, & Grunsfeld 1994; Mirabel et al. 1992; Rodríguez, Mirabel, & Martí 1992) and have therefore been described as microquasars. These characteristics make this pair of objects a subclass among the black hole candidates.

This subclass shares features with other black hole candidates. Radio jets also appear in the much brighter and spectacularly variable objects more usually called microquasars: GRS 1915+105 and GRO J1655–40 (Greiner, Morgan, & Remillard 1996; Zhang et al. 1997b), whose jets, too, are brighter and more variable. Maximum luminosities around  $3 \times 10^{37}$  ergs s<sup>-1</sup> are shared with Cygnus X-1 and the recently discovered transient GRS 1737–31 (Cui et al. 1997a). The property of being in the hard state at fairly high luminosities half the time or more is shared only with Cyg X-1. The property of having been observed only in the hard state is shared with GRS 1737–31, GS 2023+338, GRO J0422+32, and GRO J1719–24, although the total amount of time devoted to

these objects varies widely (Zhang, Cui, & Chen 1997a; Tanaka & Lewin 1995).

Despite the hard spectra of the two objects, there has been some preliminary evidence of state changes: changes in the spectral shape of 1E 1740.7–2942 above 20 keV from BATSE data (Zhang, Harmon, & Liang 1997c) and the detection of weak soft components from GRS 1758–258 (Mereghetti, Belloni, & Goldwurm 1994; Heindl & Smith 1998; Lin et al. 1999) and, with marginal significance, from 1E 1740.7–2942 (Heindl & Smith 1998).

Both sources were observed by SIGMA and ART-P to vary between observations separated by 6 months from a hard X-ray flux of about 130 mcrab (40 mcrab in the 8–20 keV ART-P band) to a level less than 10 mcrab and consistent with zero (Churazov et al. 1994; Pavlinsky et al. 1994). BATSE has also observed both 1E 1740.7–2942 and GRS 1758–258 at a near-zero flux level (Zhang et al. 1997c). Day-to-day variability is also seen in these data, including a 1 day jump in ART-P flux from 1E 1740.7–2942 from  $\sim 3$  to  $\sim 18$  mcrab. Both sources show rapid variability with a flat-topped power spectrum, behavior typical of the hard states of both black holes and neutron stars (Smith et al. 1997).

Both 1E 1740.7–2942 and GRS 1758–258 have high Galactic extinction in the optical, and counterparts have not been identified; only O stars and red supergiants have been ruled out as companions (Chen, Gehrels, & Leventhal 1994). There have therefore been no mass determinations; it has even been suggested (Bally & Leventhal 1991) that 1E 1740.7–2942 does not need a companion and could be accreting directly from a nearby molecular cloud. However, it has also been suggested that the lack of a 6.4 keV emission line in the spectrum of 1E 1740.7–2942 strongly constrains the amount of gas immediately surrounding the source (Churazov, Gilfanov, & Sunyaev 1996).

### 2. OBSERVATIONS

We have observed 1E 1740.7–2942 and GRS 1758–258 in  $\sim 1500$  s intervals with the *Rossi X-Ray Timing Explorer*

<sup>1</sup> Space Sciences Laboratory, University of California, Berkeley, Berkeley, CA 94720.

<sup>2</sup> Center for Astrophysics and Space Sciences, Code 0424, University of California, San Diego, La Jolla, CA 92093.

<sup>3</sup> NASA Goddard Space Flight Center, Code 666, Greenbelt, MD 20771.

<sup>4</sup> Department of Astronomy, University of Maryland, College Park, MD 20742.

<sup>5</sup> CEN-CEA Saclay, Service d'Astrophysique, 91191 Gif-sur-Yvette Cedex, France.

<sup>6</sup> Instituto de Astronomía, Universidad Nacional Autónoma de México, Apdo Postal 70-264, DF04510 Mexico City, Mexico.

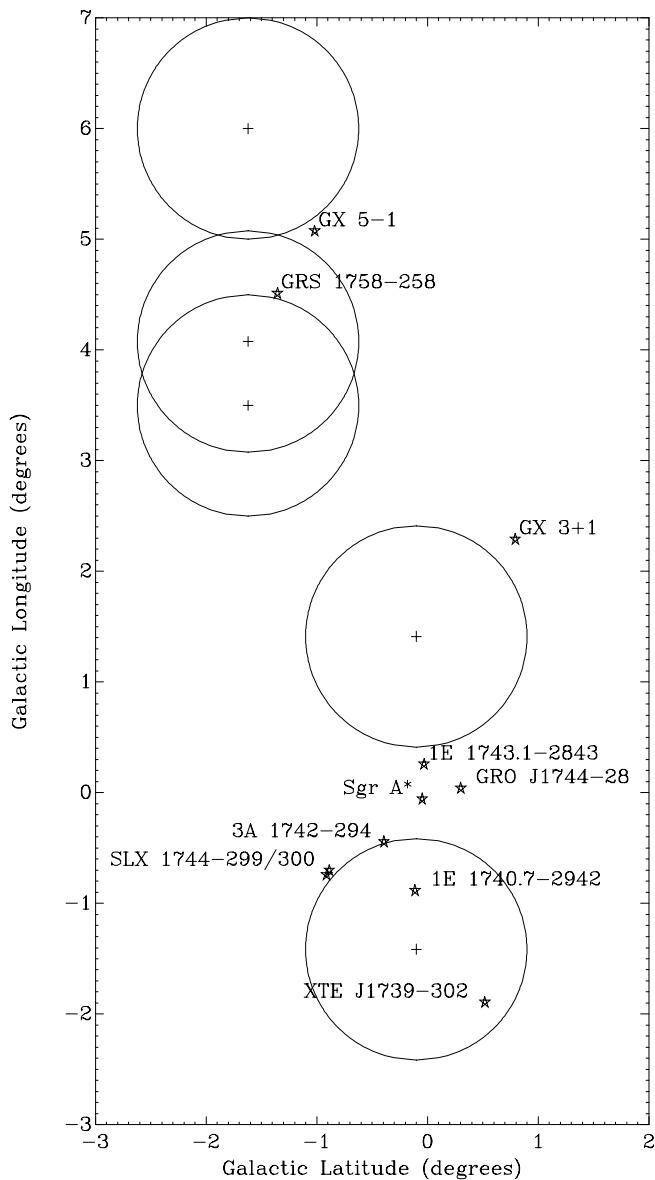


FIG. 1.—Galactic center region showing bright sources and the *RXTE* pointings used for this work. The circles shown have a radius of  $1^\circ$  near the 0% response contour for both the PCA and HEXTE instruments. The 1E 1740.7–2942 background pointing is above the 1E 1740.7–2942 source pointing on this plot; the GRS 1758–258 pointing and its backgrounds on either side are clustered near the top.

(*RXTE*). From 1996 February through October the observations were spaced 1 month apart. We have observed weekly since 1996 November. This report is based on data obtained through 1998 September. Because *RXTE* cannot point near the Sun, from late November to late January observations were not taken. All data reported here were taken with the proportional counter array (PCA).

The PCA (Jahoda et al. 1996) consists of five xenon proportional counters of  $\sim 1300 \text{ cm}^2$  each, for a total of  $6500 \text{ cm}^2$ , that are sensitive from 2 to 60 keV and share a  $1^\circ$  FWHM passively collimated field of view. We calculate instrumental background with the standard “Q6” model for consistency in a data set that spans the whole mission. Although this is not the most current model, we have found the differences among models to be negligible for these moderately bright sources. Our response matrices are those

standard to FTOOLS release 4.1, including the time dependences of the gain and of the diffusion of xenon into the propane layer.

The pointing directions were offset to avoid other nearby X-ray sources: A1742–294 and other Galactic center sources near 1E 1740.7–2942 and GX 5-1 near GRS 1758–258. The instrumental effective areas resulting from the offsets were 43% and 46% of on-axis values for 1E 1740.7–2942 and GRS 1758–258, respectively. Since both sources lie in the Galactic plane, background observations were made to determine the Galactic diffuse emission. For 1E 1740.7–2942, the background field is opposite in Galactic longitude and equal in Galactic latitude to the source field. For GRS 1758–258, the background fields are at the same Galactic latitude as the source field and on either side in Galactic longitude. The source and background fields are shown along with some bright sources in the region in Figure 1. The coordinates of these pointings are given in Smith et al. (1997).

For the spectral analyses, we used only the top layer of the PCA detectors, in the energy range 2.5–25 keV. In this mode, the diffuse X-ray background from the Galactic plane is  $77 \text{ counts s}^{-1}$  for 1E 1740.7–2942 and  $32 \text{ counts s}^{-1}$  for GRS 1758–258. The instrumental background is about  $20 \text{ counts s}^{-1}$ . Typical source count rates for both sources are about  $100 \text{ counts s}^{-1}$ . Although 1E 1740.7–2942 is somewhat brighter than GRS 1758–258 in the 2.5–25 keV band, it is also more absorbed below a few keV.

All the background-subtracted energy spectra were fitted with an absorbed power law. The time histories of the PCA count rate, the rms variability, and the photon power-law index (PLI) are shown in Figure 2. Gaps from November to January of each year are due to the *RXTE* solar pointing constraint. A few observations of each source have been removed because of very high background when the observation was made immediately after exiting the South Atlantic Anomaly. This condition occurred more often for 1E 1740.7–2942. After removing one observation of 1E 1740.7–2942 that was contaminated by the new transient XTE J1739–302 (Smith et al. 1998), we present a total of 77 observations of 1E 1740.7–2942 and 82 observations of GRS 1758–258.

### 3. SUBTLE CHANGES AND HYSTERESIS

The histories of both 1E 1740.7–2942 and GRS 1758–258 in Figure 2 clearly show that neither source turned off during the past 3 years. The count rate has ranged from about 60 to  $140 \text{ counts s}^{-1}$  in both sources.

This result is in conflict with a recent report on GRS 1758–258 by Cocchi et al. (1999) using data from the *BeppoSAX* Wide-Field Camera. They report that on three occasions (1996 September, 1997 October, and 1998 March) the flux dropped by roughly a factor of 5, becoming so low as to be undetectable. No such large drops appear in the *RXTE* data at these times, which are marked by triangles in Figure 2. Although neither the *BeppoSAX* nor the *RXTE* data are continuous, the *RXTE* data set has 59 short pointings during the range of time covered by the 16 short *BeppoSAX* observations in Cocchi et al. (1999). It is therefore highly unlikely that *RXTE* would miss the large variations reported by *BeppoSAX* if they occurred with a random distribution in time.

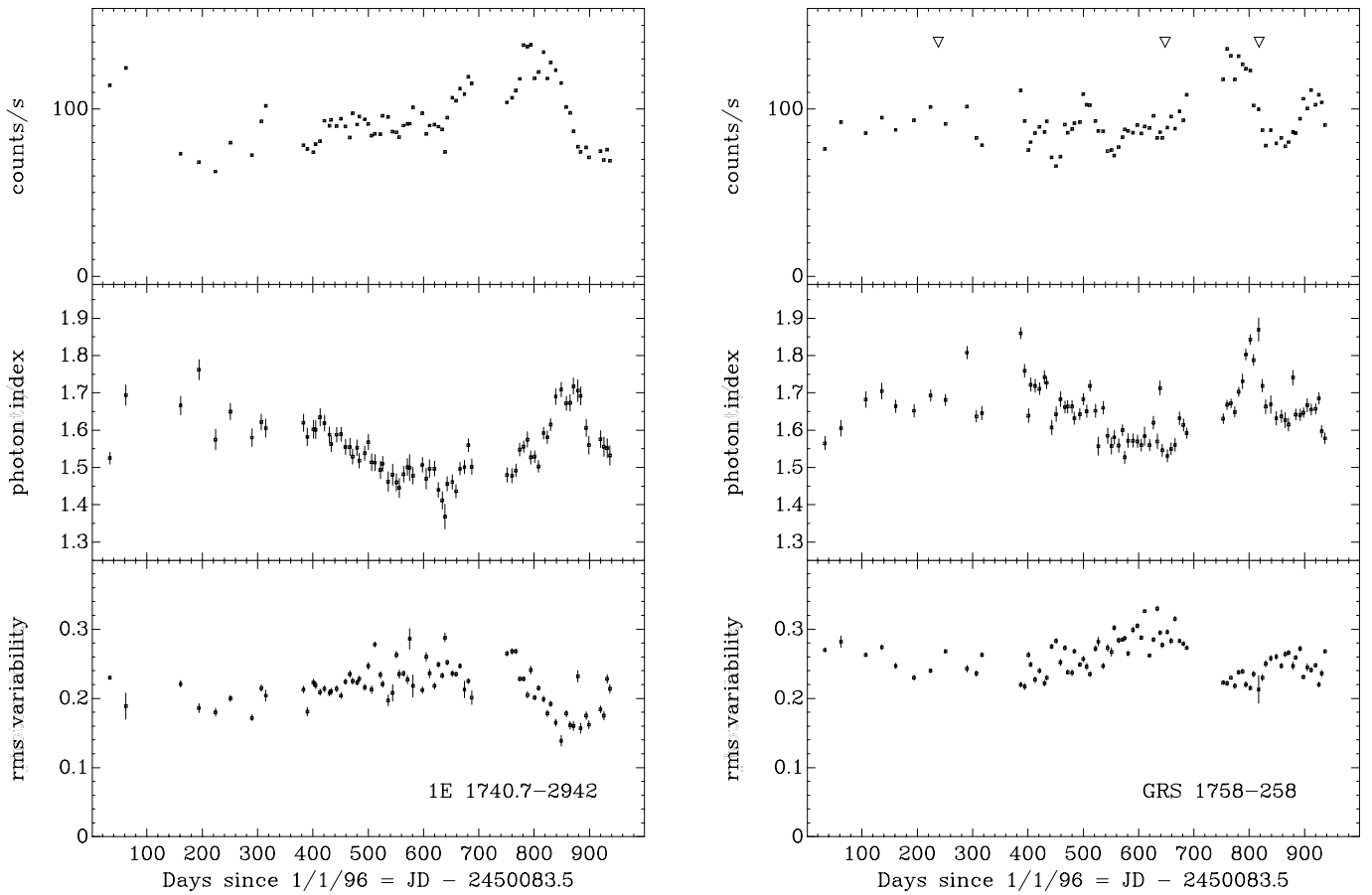


FIG. 2.—Time histories of count rate, PLI, and fractional rms variability integrated over frequency for 1E 1740.7–2942 and GRS 1758–258. In each source, the count rate and the PLI each peak at the beginning of 1998, with the PLI lagging the count rate. The approximate dates that *BeppoSax* observed drops to near-zero flux in GRS 1758–258 are marked with triangles (see § 3); the drops are not seen here.

The *RXTE* spectra show that both sources have remained in the hard state during the past 3 years, even though the PLI has occasionally softened slightly. All the variations discussed below are subtle changes within the hard state.

Both sources exhibit events of brightening and softening in early 1998 (see Fig. 2). The softening clearly lags the

brightening. By using the cross-correlation function, we found that there is a  $\sim 58$  day lag between PLI and count rate in 1E 1740.7–2942 and a  $\sim 36$  day lag in GRS 1758–258. In both sources, we used only the data around the peaks in the count rate and PLI for computing the cross-correlation function. The peaks occurred between 1998 January 22 and September 11. The brightest periods

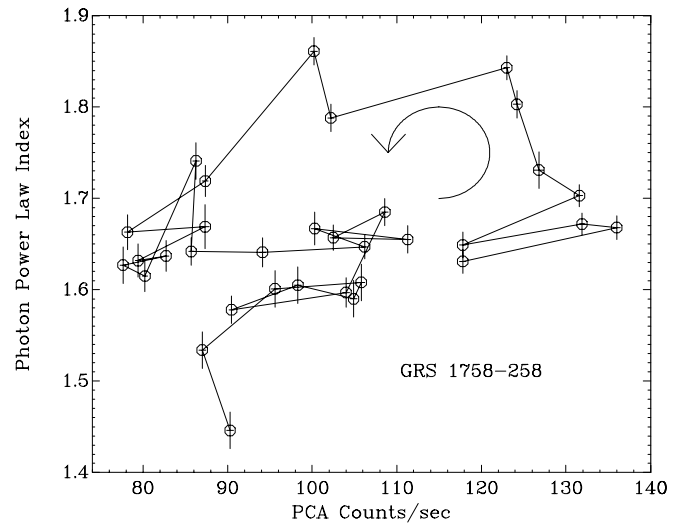
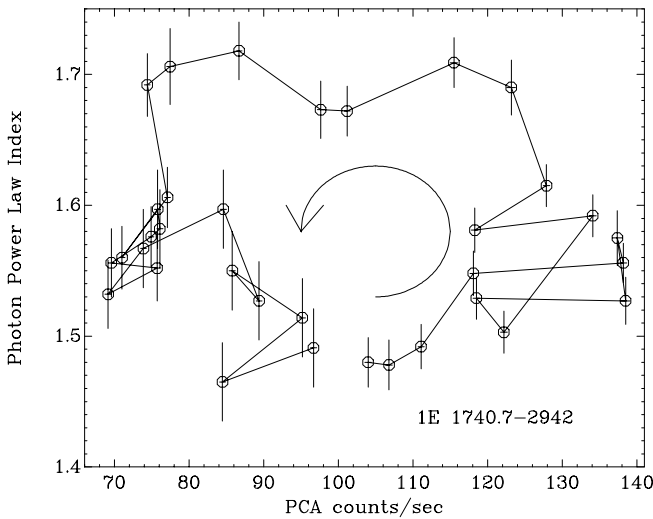


FIG. 3.—Hysteresis in 1E 1740.7–2942 and GRS 1758–258. The arrow shows the sequence of the sources’ evolution. For both the PCA count rate and PLI, only the data around the peaks were used.

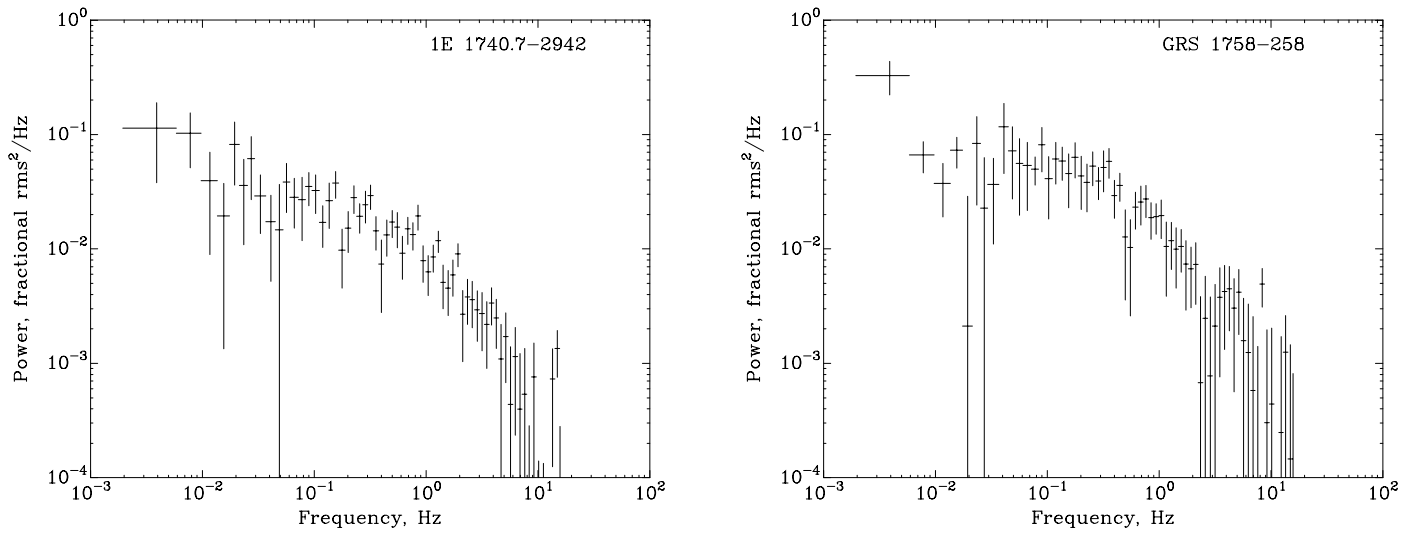


FIG. 4.—Typical power spectra for one 1500 s observation of 1E 1740.7–2942 and GRS 1758–258. It is apparent that the statistics are not good enough to observe any QPOs of the sort shown in Fig. 6. The power due to Poisson statistics has been subtracted.

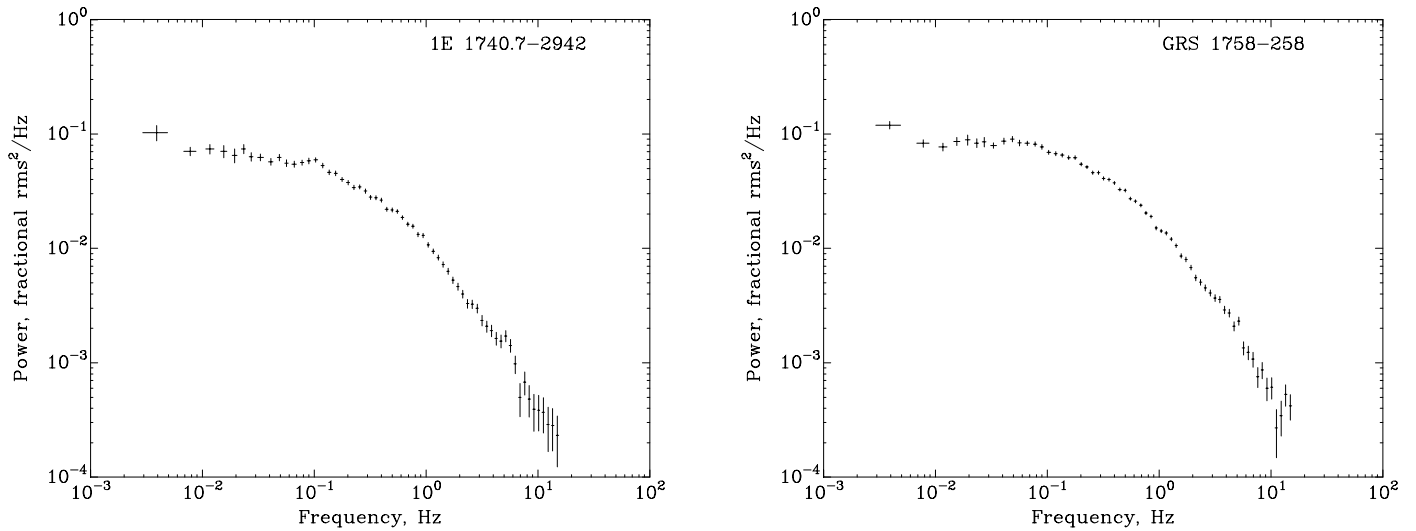


FIG. 5.—Average power spectrum of 77 observations for 1E 1740.7–2942 and 82 observations for GRS 1758–258

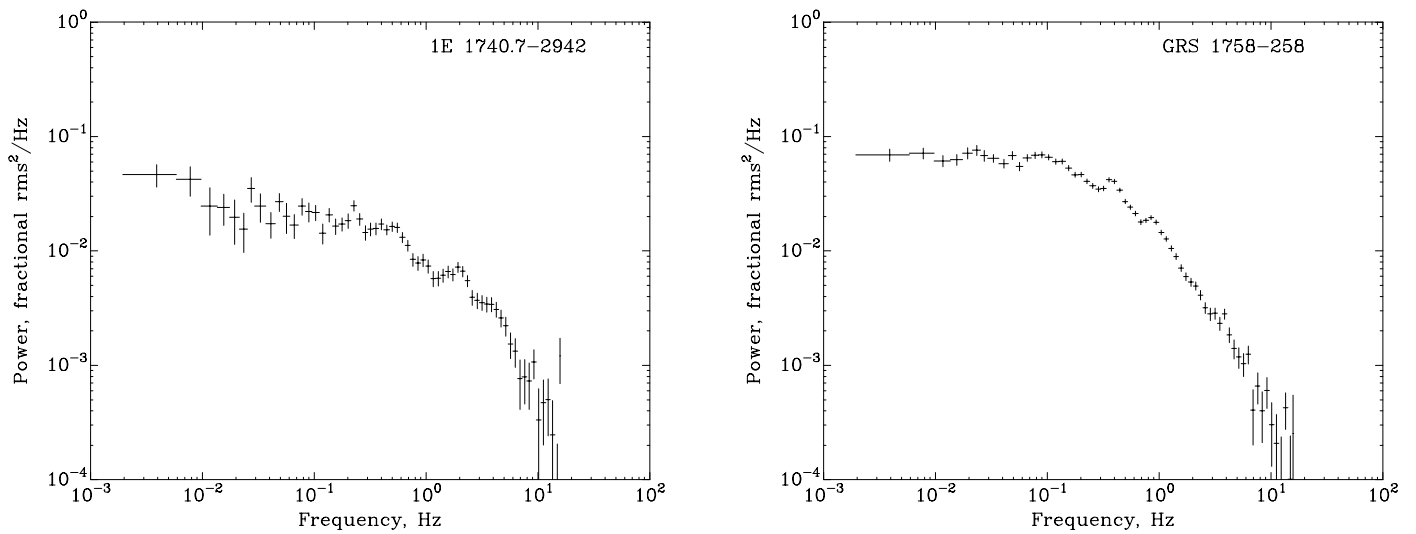


FIG. 6.—Power spectra from deep observations of 1E 1740.7–2942 and GRS 1758–258 (Smith et al. 1997). Note the QPO pairs in both black hole candidates. These QPOs are absent in the summed weekly observations (Fig. 5).

are approximately from 1998 February 2 to May 28 for 1E 1740.7–2942 and from 1998 January 22 to March 12 for GRS 1758–258.

Figure 3 shows scatter plots of PLI versus count rate for both GRS 1758–258 and 1E 1740.7–2942 during these events. When the points on the scatter plots are connected, a circle is clearly evident, showing hysteresis between the two parameters; i.e., the time lags described above can also be thought of as a phase lag of  $\sim 90^\circ$ . Because of this hysteresis effect, our data show that the time lag could hide real correlations in scatter plots using data taken over long periods.

We have considered the possibility that these events were instrumental. This is unlikely for two reasons: (1) the events are not simultaneous and (2) they are much greater changes than the known time evolution of the instrument parameters, such as efficiency and gain.

The brightening/softening event in 1E 1740.7–2942 was preceded by a period during which the PLI was gradually hardening, beginning in 1997 March and lasting for  $\sim 250$  days. In GRS 1758–258 there was also a period of gradual hardening before the similar event, lasting  $\sim 150$  days.

#### 4. TIMING RESULTS AND ANALYSIS

The counts for each observation were summed into 31.25 ms bins for the timing analysis. The individual observation times ranged from 1000 to 1500 s. Typical power spectra for GRS 1758–258 and 1E 1740.7–2942 are shown in Figure 4. The full energy range of the PCA (2–60 keV) was used for all the power spectra, but the contribution above 20 keV is small.

We fitted the power spectra with a broken power law (index 0 below the break and free above it). Typical values of the break frequency range from 0.1 to 0.8 Hz for both GRS 1758–258 and 1E 1740.7–2942. Typical values of the index above the break frequency are around  $-1$ . The rms variability integrated from 0.004 to 15.8 Hz ranged from 21.5% to 30.5% for GRS 1758–258 and from 13.9% to 28.6% for 1E 1740.7–2942.

In these short observations, the statistics were insufficient to observe any quasi-periodic oscillations (QPOs). However, in longer duration observations, QPOs have been observed in both GRS 1758–258 and 1E 1740.7–2942 (Smith et al. 1997). Figure 5 shows the average power spectrum of 77 observations for 1E 1740.7–2942 and 82 observations for GRS 1758–258, and Figure 6 shows the results from Smith et al. (1997). There are no obvious QPOs in our results. Since the QPOs exist in the long observations but do not appear when the short observations are summed, one may conclude either that the deep observations found a rare appearance of the QPOs or that the QPOs drift in frequency with time. Wijnands & van der Klis (1998) have shown a correlation between the break frequency and QPO frequency in both neutron stars and black hole candidates. Since the break frequencies of GRS 1758–258 and 1E 1740.7–2942 are variable, the QPO frequencies may also be variable.

#### 5. ENERGY SPECTRA

We fitted the energy spectra of GRS 1758–258 and 1E 1740.7–2942 with a power law absorbed by a column of neutral interstellar gas. The variations in PLI were shown

in Figure 2. For 1E 1740.7–2942, the column depth varied between  $7.4 \times 10^{22}$  and  $11 \times 10^{22}$  atoms  $\text{cm}^{-2}$  and the average value was  $9.2 \times 10^{22}$  atoms  $\text{cm}^{-2}$ . For GRS 1758–258, the absorption column varied between  $0.71 \times 10^{22}$  and  $2.3 \times 10^{22}$  atoms  $\text{cm}^{-2}$  with an average value of  $1.4 \times 10^{22}$  atoms  $\text{cm}^{-2}$ . Sheth et al. (1996) measured the column depth for 1E 1740.7–2942 at  $(8.1 \pm 0.1) \times 10^{22}$  atoms  $\text{cm}^{-2}$  with *ASCA*, which is consistent with the range we obtained. Another *ASCA* measurement (Mereghetti et al. 1997) measured the column depth for GRS 1758–258 at  $(1.5 \pm 0.1) \times 10^{22}$  atoms  $\text{cm}^{-2}$ , again consistent with our range.

The column depth is mostly determined by the spectral shape below  $\sim 4$  keV, and the PLI mostly by the higher energy part of the spectrum. At the lowest energies, we are most vulnerable to uncertainties about the influence of diffuse emission and soft sources on the edges of both fields of view (see § 2). We therefore do not claim that the range of absorption columns obtained is evidence of real variability. There is no correlation between the column depth and PLI in either source, and we are confident that the variations in PLI are real.

The PLI ranged from 1.37 to 1.76 for 1E 1740.7–2942 and from 1.45 to 1.86 for GRS 1758–258. The PLIs of 1.54 for GRS 1758–258 and 1.53 for 1E 1740.7–2942 were found by Heindl & Smith (1998). Using deep pointings in 1996 August and March, respectively. These values included HEXTE data and were derived with a model that included an exponential cutoff at high energies. With the simpler power-law model used here, the indices from the monitoring observations just before and after each deep pointing average to 1.67 and 1.68 for GRS 1758–258 and 1E 1740.7–2942, respectively. This is consistent with the expectation that, in the absence of a cutoff in the model, the effect of the cutoff will appear in a softening of the fitted PLI. The statistics in individual monitoring observations are not good enough to measure the cutoff and PLI independently.

#### 6. COMPARISON WITH CYGNUS X-1

The similarities between Cyg X-1 and 1E 1740.7–2942 and GRS 1758–258 suggest that these three sources are similar objects. Some of these similarities were mentioned in § 1: the X-ray luminosities, hard spectra, and persistent activity of all three sources. Another similarity is the shape of the power spectra. When in the hard state, all three sources show white noise up to  $\sim 0.5$  Hz (see § 4) and break to a power law, with an index above the break of  $\sim -1$ . Cyg X-1 displays a relationship between the break frequency and the rms variability integrated over frequency. This behavior was first illustrated by Belloni & Hasinger (1990). They showed that the low-state power spectrum for Cyg X-1 always had the same normalization above the break frequency, which varied. Miyamoto et al. (1992) noted that this held true from one black hole candidate to another. We searched for the same effect in GRS 1758–258 and 1E 1740.7–2942. We divided our data into three groups, those with the largest, smallest, and near-average rms and averaged the power spectra in each group. Because of this averaging, the break frequencies are more rounded than Belloni & Hasinger showed for Cyg X-1, but otherwise Figure 7 shows that GRS 1758–258 and 1E 1740.7–2942 are similar to Cyg X-1 in this respect.

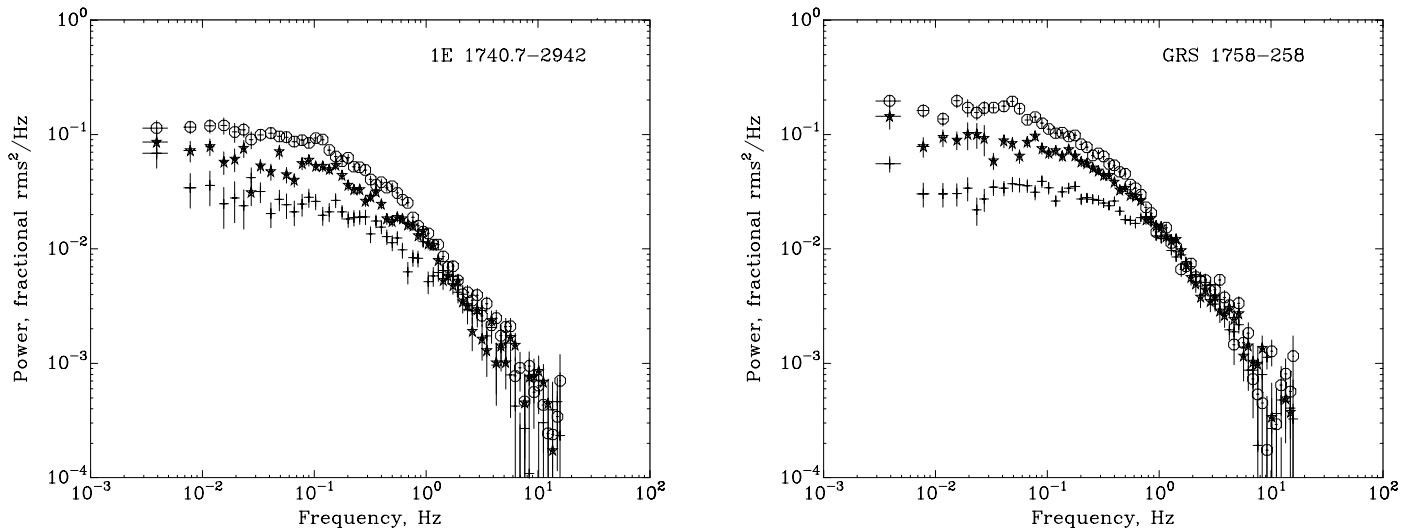


FIG. 7.—Belloni & Hasinger (1990) first found a relationship between power spectrum break frequency and integrated rms variability in Cyg X-1. This same relationship is displayed in 1E 1740.7–2942 and GRS 1758–258: the normalization is fixed above the break frequency. The power spectra with the highest frequency-integrated rms were averaged to form the top curve, the spectra with the middle rms were averaged to form the middle curve, and the spectra with the lowest rms were averaged to form the bottom curve.

Unlike 1E 1740.7–2942 and GRS 1758–258, Cyg X-1 has been observed in a true soft state, in which a soft thermal component was dominant (e.g., Cui et al. 1997b). When Cyg X-1 was in the soft state, the PLI was  $-2.2$ . A similar index was seen by BATSE above 20 keV in 1E 1740.7–2942 while that source was faint in the BATSE band (Zhang et al. 1997c). Simultaneous observations at lower energies during another occurrence of this state are needed to confirm that it is a soft state similar to that in Cyg X-1 and other black hole candidates.

## 7. DISCUSSION

### 7.1. Dynamical Model for Hysteresis

We can qualitatively explain the hysteresis or time lag between brightening and softening in 1E 1740.7–2942 and GRS 1758–258 in the context of some recent models of black hole accretion. These models (e.g., Chakrabarti & Titarchuk 1995; Esin et al. 1998) have two components in the outer regions of the flow: a standard Keplerian disk, physically thin and optically thick, and an optically thin, physically thick halo or corona. The mass in the halo is nearly in radial free fall, and it advects most of its accretion energy into the black hole rather than radiating it as the Keplerian disk does (Ichimaru 1977; Rees et al. 1982; Narayan & Yi 1995; Abramowicz et al. 1995).

In early disk-plus-corona models, the corona was produced locally by the Keplerian disk, and did not accrete independently and advectively (e.g., Liang & Price 1977; Bisnovatyi-Kogan & Blinnikov 1977). In the newer models, it is an equally valid and independent solution of the hydrodynamic equations.

Within a certain radius, the Keplerian disk is unstable, and only a very hot solution remains (an advection-dominated flow in the model of Esin et al. 1998 and a shocked flow in the model of Chakrabarti & Titarchuk 1995). The soft, thermal component of black hole candidate spectra is attributed to the inner part of the Keplerian disk,

near this boundary. The hard, power-law component is attributed to inverse Comptonization of these soft photons in the very hot inner parts of the advective flow.

While matter in the advective flow is nearly in free fall, matter in the thin disk accretes only after a gradual loss of angular momentum via viscous torques. The timescale for this process is approximately (Frank, King, & Raine 1992)

$$t_{\text{visc}} \sim 3 \times 10^5 \alpha^{-4/5} \left( \frac{\dot{M}}{10^{16} \text{ g s}^{-1}} \right)^{-3/10} \left( \frac{M}{M_{\odot}} \right)^{1/4} \times \left( \frac{R}{10^{10} \text{ cm}} \right)^{5/4} \text{ s}, \quad (1)$$

where  $M$  is the black hole mass,  $\dot{M}$  the accretion rate,  $R$  the disk radius, and  $\alpha$  the viscosity parameter ( $0 < \alpha \lesssim 1$ ). Chakrabarti & Titarchuk (1995) pointed out that if the mass accretion rate were increased at the outer edge of both flows simultaneously, it would arrive at the central regions of the advective flow first. Thus the hard component would brighten first, with the soft component brightening only after a delay approximately equal to the viscous time. We offer this delay as one explanation for the hysteresis we observe between brightening and softening. If we use  $M = 10 M_{\odot}$ ,  $\dot{M} = 10^{17} \text{ g s}^{-1}$ ,  $t_{\text{visc}}$  equal to the measured delays (see § 3), and  $\alpha = 0.3$  (Esin et al. 1998) to solve equation (1) for  $R$ , we find  $R = 5 \times 10^{10} \text{ cm}$  ( $3 \times 10^4 GM/c^2$ ) for 1E 1740.7–2942 and  $R = 3 \times 10^{10} \text{ cm}$  ( $2 \times 10^4 GM/c^2$ ) for GRS 1758–258. These disk sizes are typical of low-mass X-ray binaries accreting by Roche lobe overflow and are larger than the disks expected in systems accreting winds from massive companions (Frank et al. 1992).

### 7.2. Disk-Evaporation Model for Hysteresis

An alternative explanation for the lag between brightening and softening is quasi-static rather than dynamic: the flows can be allowed to reach an equilibrium configuration after every infinitesimal increase in accretion rate. This

explanation relies on a characteristic that is common to the models of Esin et al. (1998) and Chakrabarti & Titarchuk (1995): as the accretion rate rises, the inner edge of the Keplerian disk moves inward. If this edge were sufficiently far out to begin with, the spectral changes due to its inward advance would at first be restricted to the EUV and soft X-ray ranges, which are not observable for sources deep in the Galactic bulge. The only effect on the hard X-rays of increasing the accretion rate would be a brightening. Eventually, the disk would move in so far that it would begin to replace the hard X-ray-emitting region of the advective or shocked flow, resulting in a spectral softening.

If the response to the reduction in accretion rate back to the normal level were equally quasi-static, one would expect to see a bright and hard phase on the decline; i.e., the peaks in Figure 2 would be symmetrical in time. However, it may be that the thin disk, once established at smaller radii, takes a significant amount of time to evaporate.

It has been noted that there is hysteresis in the hard/soft/hard transitions of soft X-ray transients (Miyamoto et al. 1995). In a typical outburst of this class of black hole candidate, the system remains in the hard state as the luminosity rises quickly from quiescence to near maximum, then switches to the soft state, then returns to the hard state only when the luminosity is on the order of 1% of the maximum. The quick rise in accretion rate and quick transition to the soft state are thought to be due to the rapid propagation of a thermal-ionization instability in the disk (Cannizzo, Wheeler, & Ghosh 1985). This mechanism is not relevant to 1E 1740.7–2942 and GRS 1758–258, since their usual accretion rates are high enough that the disk would remain ionized by the X-rays from the central regions of the accretion flow.

The return of the transients to the hard state, however, may be relevant to our observations. Mineshige (1996) interpreted this return as a transition from a Keplerian disk to an advective flow. Both the disk and advective flows are stable over most of the accretion rates traversed during the decline, but the transition does not take place until the disk solution becomes unstable at very low accretion rates. In other words, the disk, once it is established, tends to persist in regimes where both solutions are stable.

The typical luminosity of both 1E 1740.7–2942 and GRS 1758–258 is  $2 \times 10^{37}$  ergs  $s^{-1}$  from 1 to 200 keV (Heindl & Smith 1998). Our data never deviate by more than about 50% from this value. This is roughly 1%–7% of the Eddington luminosity for black holes of 3–20  $M_{\odot}$  and is

orders of magnitude higher than the luminosity where the idealized transient of Mineshige (1996) is forced to return to the hard state. Nonetheless, if the added regions of the inner disk in the transients persist for a month or more at accretion rates where the advective flow would also be stable, then the more modest inward extensions of the disk that occur when 1E 1740.7–2942 and GRS 1758–258 brighten might persist as long. The time asymmetry in our data, in this interpretation, would be due to the evaporation time of the inner disk being longer than the time in which the accretion rate returns to normal.

## 8. CONCLUSIONS

We have presented the most detailed long-term coverage of these black hole candidates to date. In this 3 yr period, we have never seen either source at a flux level less than half its maximum. Although neither source has entered the soft (high) state in this time, we have seen variations in spectral index within the range usually associated with the hard or low state (photon  $PLI < 2.0$ ).

There is hysteresis when GRS 1758–258 and 1E 1740.7–2942 brighten and soften within the hard state, with the softening lagging the brightening by 1–2 months. This hysteresis could be due to the different propagation times in a disk and halo of an increase in  $\dot{M}$  (§ 7.1), or else to a persistence of the thin disk after  $\dot{M}$  returns to normal (§ 7.2). If the former is the correct interpretation, the lag time implies accretion disks of the size usually associated with accretion from a low-mass companion overflowing its Roche lobe.

We find that the weekly observations of GRS 1758–258 and 1E 1740.7–2942 reveal no QPOs when summed up over many weeks. This leads us to the conclusion either that our deep observations observed rare appearances of the QPOs or, more likely, that they drift in frequency with time, consistent with the behavior described by Wijnands & van der Klis (1998) for other sources. Both objects show the same relationship between the break frequency of the power spectrum and the total rms variability as other hard-state sources.

We would like to thank Ann Esin, Lars Bildsten, and Lev Titarchuk for useful discussions on the interpretation of the hysteresis results. This work was supported by NASA grants NAG 5-4110, NAG 5-7522, and NAG 5-7265.

## REFERENCES

- Abramowicz, M. A., Chen, X., Kato, S., Lasota, J. P., & Regev, O. 1995, *ApJ*, 438, L37
- Bally, J., & Leventhal, M. 1991, *Nature*, 353, 234
- Belloni, T., & Hasinger, G. 1990, *A&A*, 227, L33
- Bisnovatyi-Kogan, G. S., & Blinnikov, S. I. 1977, *A&A*, 59, 111
- Cannizzo, J. K., Wheeler, J. C., & Ghosh, P. 1985, in *Proc. Cambridge Workshop, Cataclysmic Variables and Low-Mass X-Ray Binaries*, ed. D. Q. Lamb & J. Patterson (Dordrecht: Reidel), 307
- Chakrabarti, S. K., & Titarchuk, L. G. 1995, *ApJ*, 455, 623
- Chen, W., Gehrels, N., & Leventhal, M. 1994, *ApJ*, 426, 586
- Churazov, E., Gilfanov, M., & Sunyaev, R. 1996, *ApJ*, 464, L71
- Churazov, E., et al. 1994, *ApJS*, 92, 381
- Cocchi, M., et al. 1999, in *Proc. 3rd INTEGRAL Workshop, The Extreme Universe*, ed. G. Palumbo, A. Bazzano, & C. Winkler (Noordwijk: ESA-ESTEC), in press
- Cui, W., Heindl, W. A., Swank, J. H., Smith, D. M., Morgan, E. H., Remillard, R., & Marshall, F. E. 1997a, *ApJ*, 487, L73
- Cui, W., Zhang, S. N., Focke, W., & Swank, J. H. 1997b, *ApJ*, 484, 383
- Esin, A., Narayan, R., Cui, W., Grove, J. E., & Zhang, S. N. 1998, *ApJ*, 505, 854
- Frank, J., King, A., & Raine, D. 1992, *Accretion Power in Astrophysics* (2d ed.; Cambridge: Cambridge Univ. Press), 99
- Greiner, J., Morgan, E. H., & Remillard, R. A. 1996, *ApJ*, 473, L107
- Heindl, W. A., et al. 1993, *ApJ*, 408, 507
- Heindl, W. A., Prince, T., & Grunsfeld, J. 1994, *ApJ*, 430, 829
- Heindl, W. A., & Smith, D. M. 1998, *ApJ*, 506, L35
- Ichimaru, S. 1977, *ApJ*, 214, 840
- Jahoda, K., et al. 1996, *Proc. SPIE*, 2808, 59
- Liang, E. P. T., & Price, R. H. 1977, *ApJ*, 218, 247
- Lin, D., et al. 1999, *ApJ*, in press
- Mereghetti, S., Belloni, T., & Goldwurm, A. 1994, *ApJ*, 433, L21
- Mereghetti, S., Cremonesi, D. I., Haardt, F., Murakami, T., Belloni, T., & Goldwurm, A. 1997, *ApJ*, 476, 829
- Mineshige, S. 1996, *PASJ*, 48, 93
- Mirabel, I., et al. 1992, *Nature*, 358, 215
- Miyamoto, S., Kitamoto, S., Hayashida, K., & Egoshi, W. 1995, *ApJ*, 442, L13
- Miyamoto, S., Kitamoto, S., Iga, S., Negoro, H., & Terada, K. 1992, *ApJ*, 391, L21
- Narayan, R., & Yi, I. 1995, *ApJ*, 452, 710

- Pavlinsky, M. N., et al. 1994, ApJ, 425, 110
- Rees, M. J., Begelman, M. C., Blandford, R. D., & Phinney, E. S. 1982, Nature, 275, 17
- Rodríguez, L. F., Mirabel, I. F., & Martí, J. 1992, ApJ, 401, L15
- Sheth, S., Liang, E., Luo, C., & Murakami, T. 1996, ApJ, 468, 755
- Smith, D. M., Heindl, W. A., Swank, J., Leventhal, M., Mirabel, I. F., & Rodríguez, L. F. 1997, ApJ, 489, L51
- Smith, D. M., et al. 1998, ApJ, 501, L181
- Sunyaev, R., et al. 1991, ApJ, 383, L49
- Tanaka, Y., & Lewin, W. H. G. 1995, in X-Ray Binaries, ed. W. H. G. Lewin, J. van Paradijs, & E. P. J. van den Heuvel (Cambridge: Cambridge Univ. Press), 126
- Wijnands, R., & van der Klis, M. 1999, ApJ, 514, 939
- Zhang, S. N., Cui, W., & Chen, W. 1997a, ApJ, 482, L155
- Zhang, S. N., et al. 1997b, ApJ, 479, 381
- Zhang, S. N., Harmon, B. A., & Liang, E. P. 1997c, in AIP Conf. Proc. 410, Proc. 4th Compton Symp., Part 2, ed. C. D. Dermer, M. S. Strickman, & J. D. Kurfess (New York: AIP), 873